



ELSEVIER

journal homepage: www.elsevier.com/locate/febsopenbio

NADH oxidase and alkyl hydroperoxide reductase subunit C (peroxiredoxin) from *Amphibacillus xylanus* form an oligomeric assembly



Toshiaki Arai^{a,1}, Shinya Kimata^{a,1}, Daichi Mochizuki^a, Keita Hara^a, Tamotsu Zako^b, Masafumi Odaka^b, Masafumi Yohda^b, Fumio Arisaka^c, Shuji Kanamaru^c, Takashi Matsumoto^d, Shunsuke Yajima^a, Junichi Sato^a, Shinji Kawasaki^a, Youichi Niimura^{a,*}

^a Department of Bioscience, Tokyo University of Agriculture, Tokyo, Japan

^b Department of Biotechnology and Life Science, Tokyo University of Agriculture and Technology, Tokyo, Japan

^c Department of Life Science, Tokyo Institute of Technology, Kanagawa, Japan

^d X-ray Research Laboratory, Rigaku Corporation, Tokyo, Japan

ARTICLE INFO

Article history:

Received 28 November 2014

Revised 23 January 2015

Accepted 23 January 2015

Keywords:

Amphibacillus xylanus

NADH oxidase

AhpC (Prx)

Protein interaction

Ionic strength

ABSTRACT

The NADH oxidase–peroxiredoxin (Prx) system of *Amphibacillus xylanus* reduces hydroperoxides with the highest turnover rate among the known hydroperoxide-scavenging enzymes. The high electron transfer rate suggests that there exists close interaction between NADH oxidase and Prx. Variant enzyme experiments indicated that the electrons from β -NADH passed through the secondary disulfide, Cys128–Cys131, of NADH oxidase to finally reduce Prx. We previously reported that ionic strength is essential for a system to reduce hydroperoxides. In this study, we analyzed the effects of ammonium sulfate (AS) on the interaction between NADH oxidase and Prx by surface plasmon resonance analysis. The interaction between NADH oxidase and Prx was observed in the presence of AS. Dynamic light scattering assays were conducted while altering the concentration of AS and the ratio of NADH oxidase to Prx in the solutions. The results revealed that the two proteins formed a large oligomeric assembly, the size of which depended on the ionic strength of AS. The molecular mass of the assembly converged at approximately 300 kDa above 240 mM AS. The observed reduction rate of hydrogen peroxide also converged at the same concentration of AS, indicating that a complex formation is required for activation of the enzyme system. That the complex generation is dependent on ionic strength was confirmed by ultracentrifugal analysis, which resulted in a signal peak derived from a complex of NADH oxidase and Prx (300 mM AS, NADH oxidase: Prx = 1:10). The complex formation under this condition was also confirmed structurally by small-angle X-ray scattering.

© 2015 The Authors. Published by Elsevier B.V. on behalf of the Federation of European Biochemical Societies. This is an open access article under the CC BY-NC-ND license (<http://creativecommons.org/licenses/by-nc-nd/4.0/>).

1. Introduction

Amphibacillus xylanus exhibits the same growth rate and cell yield under both anaerobic and aerobic conditions despite lacking a respiratory system and heme-catalase [1]. This is due to the presence of anaerobic and aerobic pathways that produce similar

Abbreviations: Nox, NADH oxidase; AhpC (Prx), peroxiredoxin; AS, ammonium sulfate; SPR, surface plasmon resonance; DLS, dynamic light scattering; AUC, analytical ultracentrifugation; SAXS, small-angle X-ray scattering

* Corresponding author at: The Department of Bioscience, Tokyo University of Agriculture, 1-1-1 Sakuragaoka, Setagayaku, Tokyo 156-8502, Japan. Tel./fax: +81 3 54772764.

E-mail address: niimura@nodai.ac.jp (Y. Niimura).

¹ Toshiaki Arai and Shinya Kimata contributed equally to this research and are co-first authors.

amounts of ATP [2]. The oxygen metabolic enzyme in *A. xylanus*, NADH oxidase [3], which catalyzes the reduction of oxygen to hydrogen peroxide with β -NADH, can also reduce hydrogen peroxide to water in the presence of AhpC (Prx) protein, a member of the peroxiredoxin (Prx) family [4,5]. NADH oxidase thus belongs to a family of peroxiredoxin (Prx) oxidoreductases, which also includes alkyl hydroperoxide reductase F (AhpF) [4,5]. The NADH oxidase–Prx system is believed to play an important role in peroxide scavenging and the effective regeneration of NAD^+ to maintain redox balance in the cells of *A. xylanus* [5,6]. The systems are widely distributed in bacterial obligate aerobes, facultative aerobes, aero-tolerant anaerobes, and obligate anaerobes [7]. NADH oxidase is a homodimer composed of 55 kDa subunits, each containing 1 mol of FAD [8]. The amino acid sequence of NADH oxidase exhibits

<http://dx.doi.org/10.1016/j.fob.2015.01.005>

2211-5463/© 2015 The Authors. Published by Elsevier B.V. on behalf of the Federation of European Biochemical Societies. This is an open access article under the CC BY-NC-ND license (<http://creativecommons.org/licenses/by-nc-nd/4.0/>).

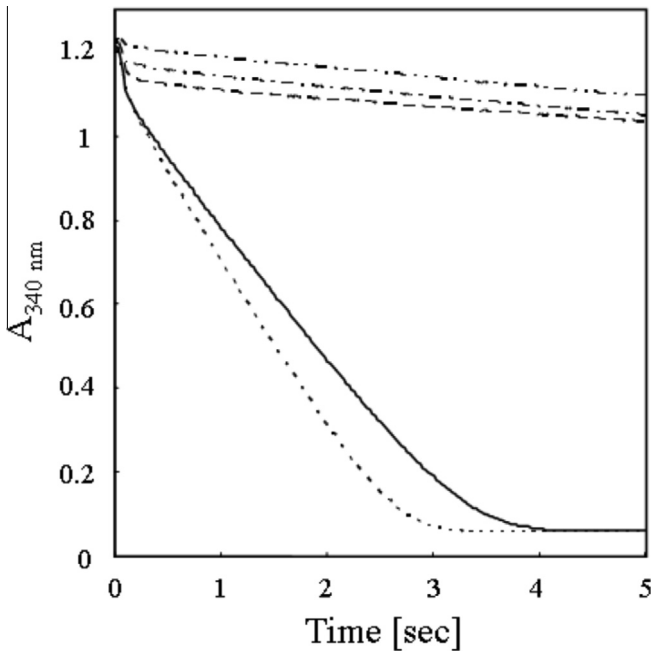


Fig. 1. Time course for the oxidation of NADH by hydrogen peroxide in the presence of Prx plus wild-type and variant C128S, C131S, C128S/C131S, and C480S NADH oxidases. The activities were measured under aerobic conditions at 25 °C. 0.56 μM *A. xylanus* NADH oxidase (solid line), variant C128S (dashed line), variant C131S (dashed-dotted line), variant C128S/C131S (dashed-dotted line), or variant C480S (dotted line), and 35.2 μM Prx were mixed with 50 mM sodium phosphate buffer (pH 7.0) containing 0.5 mM EDTA, 0.5 mM hydrogen peroxide, 200 μM NADH, and 300 mM AS and monitored at 340 nm.

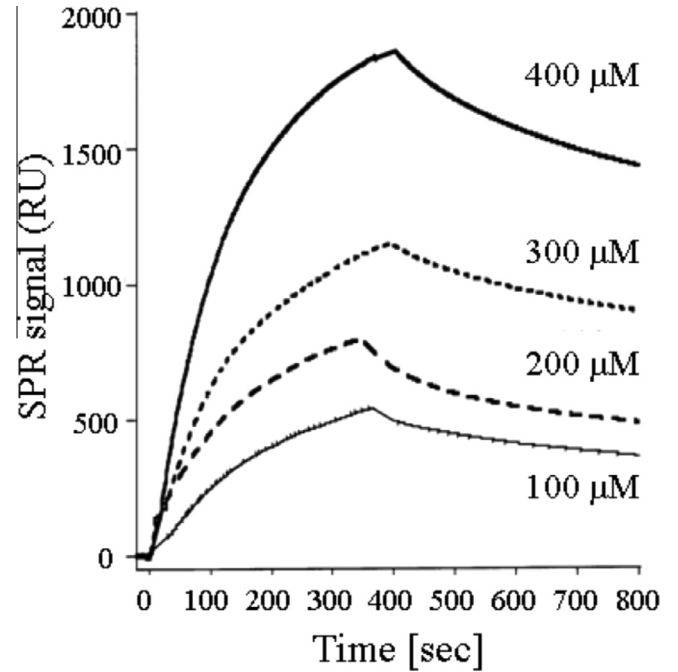


Fig. 3. NADH oxidase-Prx interaction kinetics determined by surface plasmon resonance (SPR). Prx was immobilized on the dextran matrix of a CM5 chip. NADH oxidase-Prx interaction at pH 7.0 was analyzed by injecting different concentrations of NADH oxidase in the presence of 100 mM AS. RU: response units.

51.2% shared identity with AhpF from *Salmonella typhimurium* [3,9]. The K_m values of both enzymes for the substrates hydrogen peroxide and cumene hydroperoxide are too low to determine using the employed analytical methods [4]. The turnover numbers of the peroxide reductions catalyzed by both enzymes are

extremely high compared with those of other known peroxide-scavenging enzymes [10–16]. While two distinct proteins take part in the reaction, the NADH oxidase-Prx system can nevertheless reduce hydroperoxides at a similar rate constant for the first step of the enzyme reaction [10], suggesting that NADH oxidase and Prx interact very closely to reduce hydroperoxides. In this report, we investigated the protein interaction between NADH oxidase and Prx from *A. xylanus*.

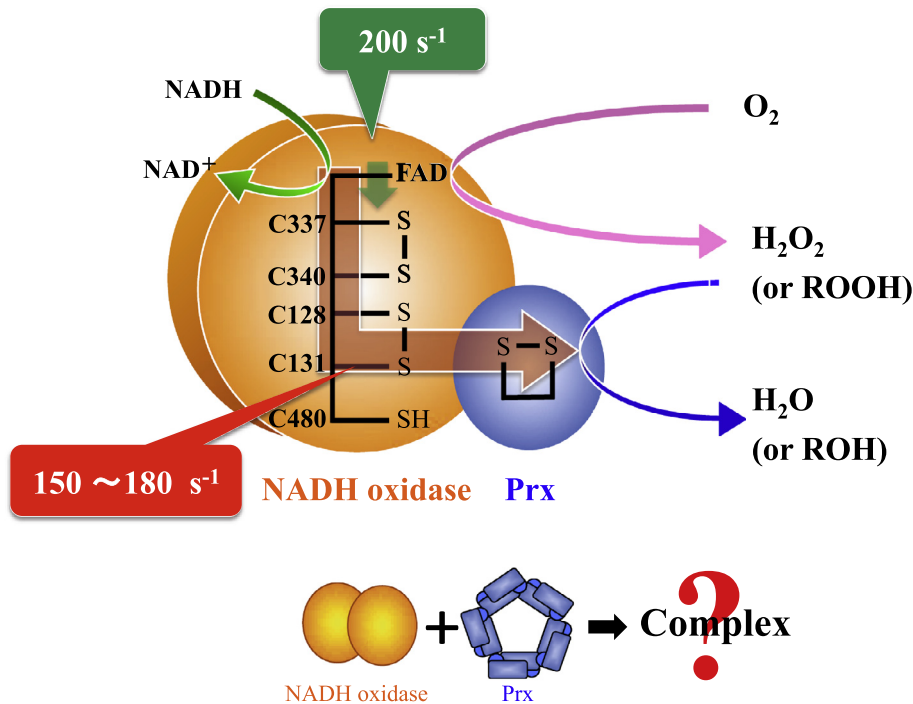


Fig. 2. The proposed reaction mechanism of the NADH oxidase-Prx system.

Table 1

Kinetic and affinity constants for the binding of NADH oxidase to Prx. NADH oxidase–Prx interaction was analyzed by injecting different concentrations of NADH oxidase in the presence of 100 mM AS.

	k_{on} ($M^{-1} S^{-1}$)	k_{off} (S^{-1})	K_d (μM)
NADH oxidase	29 ± 13	$6.3 \times 10^{-4} \pm 1.0 \times 10^{-4}$	24 ± 7

2. Results and discussion

2.1. Hydrogen peroxide reductase activity of variant NADH oxidases

NADH oxidase has two disulfide bonds, Cys337–Cys340 and Cys128–Cys131, and one cysteine residue, Cys480, as candidate redox centers, in addition to enzyme-bound FAD that receives elec-

trons directly from β -NADH [17]. A comparison of kinetics and spectral titrations of both wild and variant NADH oxidases indicated that electrons from enzyme-bound FADH₂ are passed to the disulfide bond, Cys337–Cys340 [8,10,17]. In contrast, it is unclear whether the second disulfide, Cys128–Cys131, or a free cysteine residue, Cys480, is involved in the electron flow for peroxide reductions [10]. We constructed four variant NADH oxidases, C128S, C131S, C128S/C131S, and C480S, in which Cys-128, Cys-131, and Cys-480 were changed to a serine residue. The catalytic activity of the four variant enzymes was examined by steady-state kinetics. The hydrogen peroxide reductase activity of the variant enzyme, C480S, did not differ from that of wild-type, so Cys-480 does not engage in the electron transfer of NADH oxidase to Prx (Fig. 1). Little activity was observed in variant enzymes lacking Cys-128, Cys-131, or both cysteine residues under a sufficient concentration of Prx, indicating

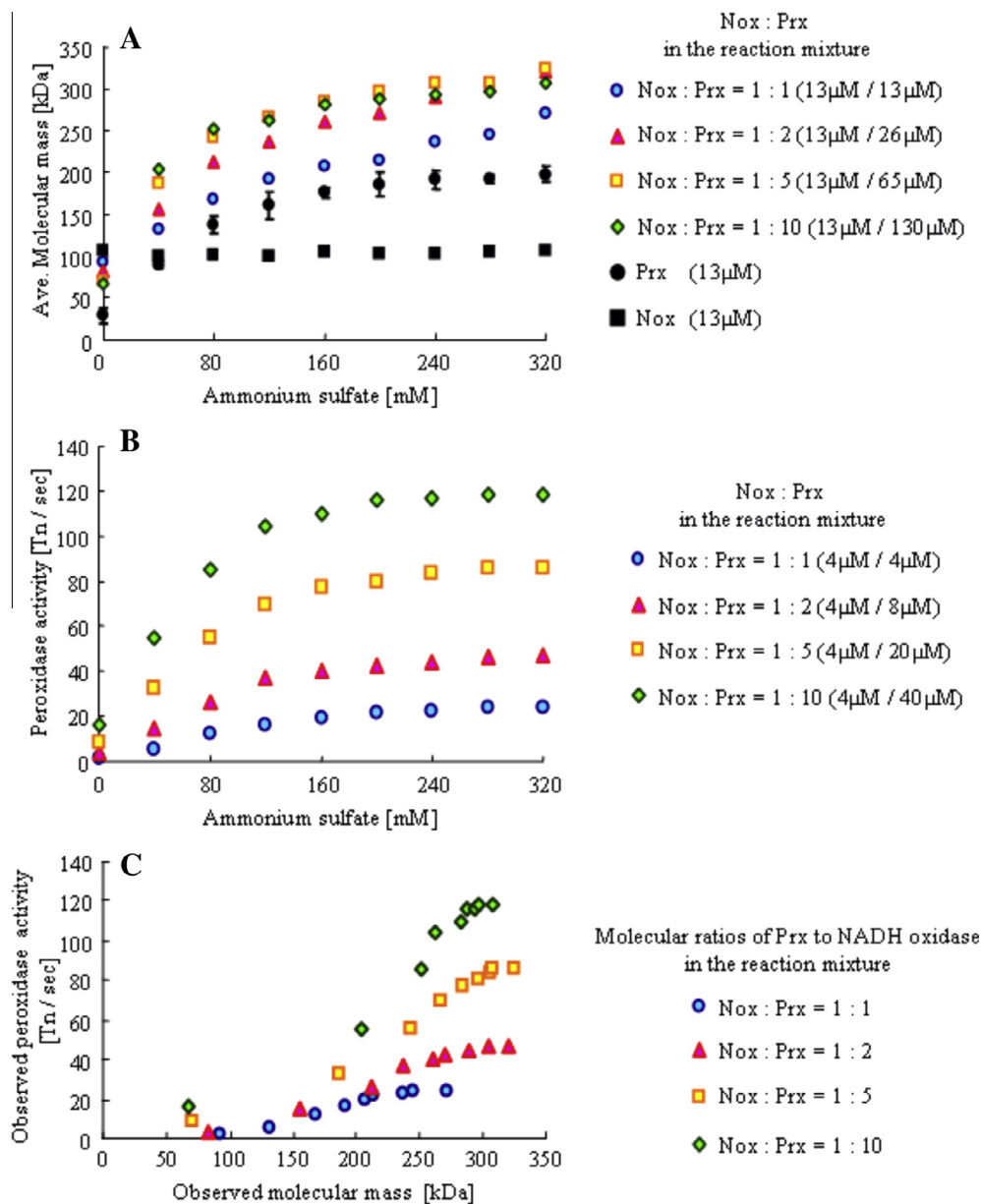


Fig. 4. Molecular mass and hydrogen peroxide reductase activity in the mixture of NADH oxidase and Prx under various concentrations of AS. (A) Molecular mass of NADH oxidase, Prx, and their mixtures. Measurements were performed by dynamic light scattering (DLS) at 25 °C under various concentrations of AS (0 – 320 mM). The ratios in the mixture of NADH oxidase and Prx were 1:1, 2, 5, and 10 (subunit per subunit). (B) Hydrogen peroxide reductase activity in the mixtures of NADH oxidase and Prx. The activities were measured under anaerobic conditions at 25 °C with 50 mM sodium phosphate buffer (pH 7.0) containing 0.5 mM EDTA, 0.5 mM hydrogen peroxide, 200 μM NADH, and 0–320 mM AS. (C) The correlation between molecular mass and activity was deduced from (A) and (B).

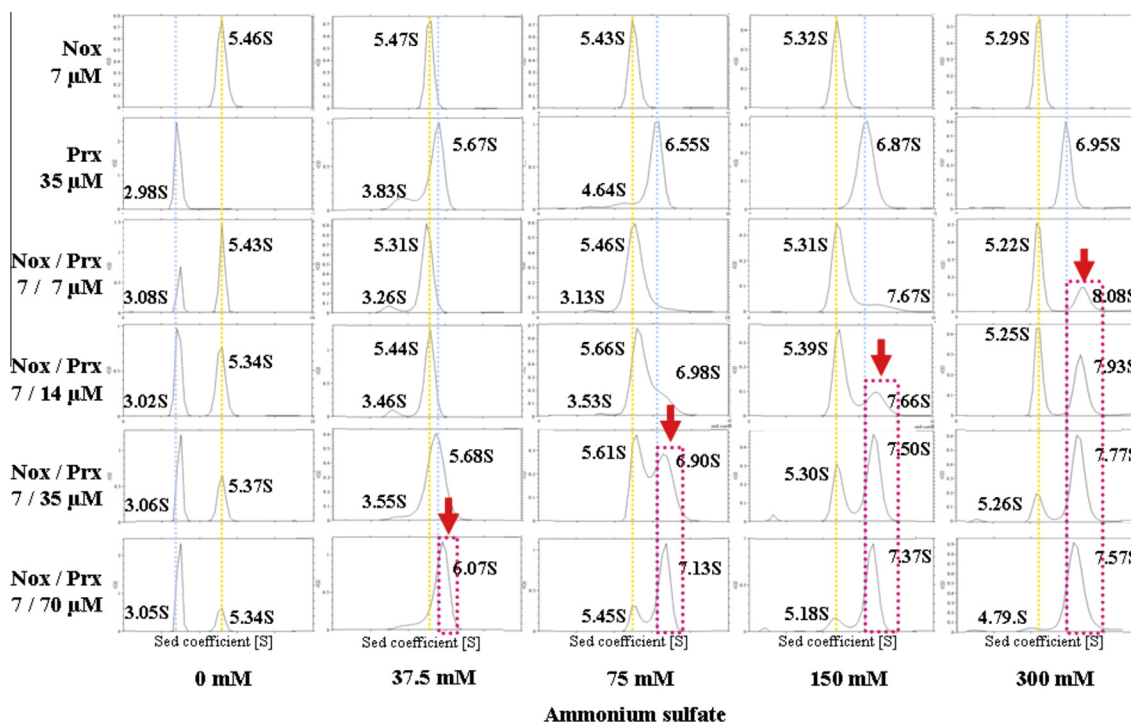


Fig. 5. The oligomerization states of the complex in various mixing ratios of NADH oxidase and Prx. The sedimentation velocity analysis was performed at 20 °C. The peaks of NADH oxidase (yellow dotted-lines), Prx (blue dotted-lines), and their complex (red dotted-lines) under various concentrations of AS (0–300 mM) were monitored at an absorbance of 280 nm. The sedimentation velocity data were analyzed using the SEDFIT program [27]. (For interpretation of the references to color in this figure legend, the reader is referred to the web version of this article.)

that electrons from the second disulfide, Cys128–Cys131, pass through the disulfide of Prx to finally reduce peroxides. Thus, it is suspected that the sequence of reducing reactions in the NADH oxidase–Prx system is $\text{NADH} \rightarrow \text{enzyme-bound FAD} \rightarrow \text{Cys337–Cys340} \rightarrow \text{Cys128–Cys131} \rightarrow \text{Prx} \rightarrow \text{H}_2\text{O}_2$ (or ROOH) (Fig. 2), which is consistent with the findings for the AhpF–AhpC (Prx) system from *S. typhimurium* [18,19]. Despite the four redox centers composed of two individual proteins, the NADH oxidase–Prx system catalyzes reduction of hydroperoxides with a V_{max} value of 150–180 s^{-1} [4]. Because the reduction rate of enzyme-bound FAD (200 s^{-1}) by β -NADH is similar to that of peroxidase reductions [10], the transfer of electrons from Cys128–Cys131 to Prx should progress rapidly. Therefore, it is assumed important that NADH oxidase and Prx interact very closely with each other.

2.2. Protein interaction analysis by surface plasmon resonance (SPR)

The hydroperoxide reductase activity of the NADH oxidase–Prx system is dependent on ionic strength [4]. Its activity is accelerated regardless of the type of inorganic ions, and ammonium sulfate (AS) is the most effective in stabilizing the activity among the various salts tested [4]. High hydroperoxide reductase activities of the enzyme system were observed under an optimal concentration of AS (150–300 mM) [4,20]. We investigated the protein interaction between NADH oxidase and Prx in the absence or presence of AS by surface plasmon resonance (SPR). The SPR signal obtained in the absence of AS was unstable, whereas interaction between both proteins was visible in the presence of 100 mM AS (Fig. 3). The dissociation constant (K_d) of NADH oxidase for Prx was determined to be $24 \pm 7 \mu\text{M}$ in this condition (Table 1). In order to observe the protein interaction state between NADH oxidase and Prx that is dependent on ionic strength, this protein mixture was applied to a gel-filtration column with 300 mM AS. We could not, however, find any signal peak consistent with an assembly composed of

these proteins. It is presumed that the NADH oxidase–Prx assembly dissociated into two distinct proteins under a condition of flux, such as a gel-filtration column. In the next section, we performed a dynamic light scattering analysis under static conditions.

2.3. Protein interaction analysis by dynamic light scattering (DLS)

In our previous report, a preliminary X-ray crystallography analysis gave information that *A. xylanus* Prx forms a decamer (PDB code: 1WE0) [20,21]. We also observed that the oligomeric state of Prx is significantly affected by the ionic strength of the solution [20]. In the end, its molecular mass reached approximately 200 kDa, equivalent to a decamer at the ionic strength above 300 mM (100 mM AS) by DLS assay [20]. We also confirmed that Prx formed a decamer that was dependent on ionic strength through DLS measurement (Fig. 4A). On the other hand, NADH oxidase formed a dimer (approximately 100 kDa) with no relation to ionic strength in the absence of Prx.

Investigations into NADH oxidase–Prx complex formation were conducted in the AS range from 0 mM to 320 mM using protein solutions mixed with NADH oxidase and Prx in various ratios from 1:1 to 1:10 (subunit per subunit). In the absence of AS, little hydrogen peroxide reductase activity was observed in all mixtures and also when the average molecular mass was under 100 kDa, suggesting that NADH oxidase and Prx form hardly any complex at low ionic strength (Fig. 4B). In contrast, by increasing the concentration of AS from 0 mM to 320 mM, both the hydrogen peroxide reductase activity and the average molecular mass were increased, depending on ionic strength. The molecular mass in the solutions finally converged at approximately 300 kDa above 240 mM AS. The observed hydrogen peroxide reductase activity also converged at the same concentration of AS (Fig. 4C). The results of DLS confirmed those of SPR measurements and indicated that complex formation is required for activation of the NADH oxidase–Prx system.

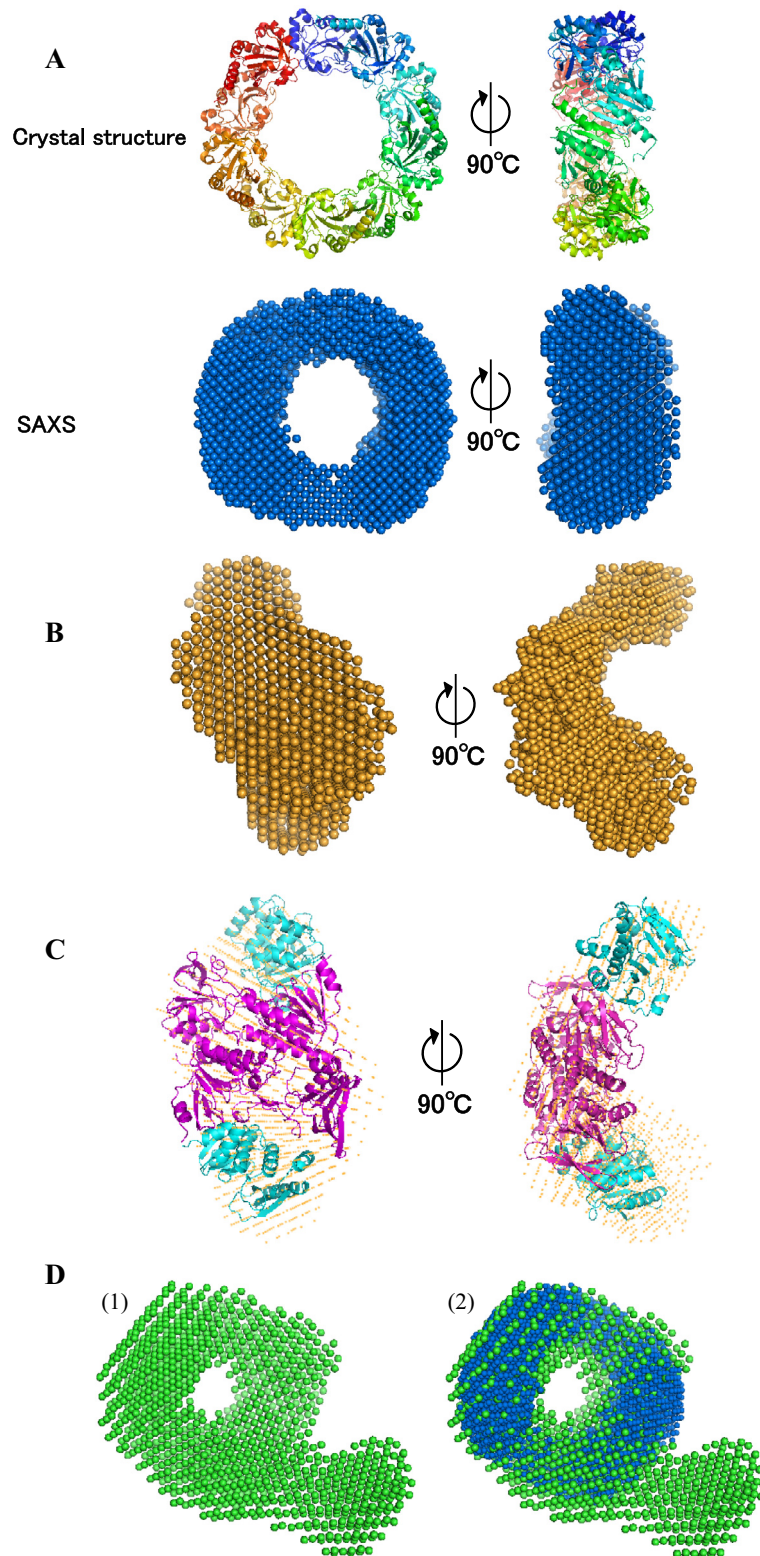


Fig. 6. The solution structures of Prx, NADH oxidase and their complex. The solution structures of Prx, NADH oxidase and their complex at 14.3 mg/mL containing 300 mM AS were determined by small-angle X-ray scattering (SAXS). Each protein was reconstructed through an ensemble of dummy residues (C- α atoms of amino acid residues) based on the scattering curves derived from proteins. (A) The solution structure of *A. xylanus* Prx (below) is shown with the crystal structure of decameric *A. xylanus* Prx (above, PDB code: 1WE0). (B) The solution structure of *A. xylanus* NADH oxidase. (C) A probable model of NADH oxidase was built using a crystal structure of AhpF (PDB code: 1HYU). An NTD domain (cyan) and C-terminal portion (magenta) of AhpF was docked into the SAXS image of NADH oxidase (B), and an NTD domain was moved manually to fit into it. (D-1) The solution structure of NADH oxidase-Prx complex was obtained by analyzing the solution mixed with a ratio of NADH oxidase and Prx equal to 1:10 (subunit per subunit). (D-2) The solution structure of Prx (blue) was manually superimposed on that of the complex (green) using the Coot program. (For interpretation of the references to color in this figure legend, the reader is referred to the web version of this article.)

2.4. Protein interaction analysis by analytical ultracentrifugation (AUC)

The results of DLS measurement indicated that an oligomeric assembly estimated at approximately 300 kDa was formed in the mixture of NADH oxidase and Prx at the AS concentration above 240 mM. Because the observed molecular mass was an average value in the protein mixture, the oligomerization states of the complex in various mixing ratios of NADH oxidase and Prx were analyzed by analytical ultracentrifugation (AUC), with the absorbance at 280 nm and AS concentration from 0 mM up to 300 mM (Fig. 5). Initially, it may appear odd to see only two peaks in $c(s)$ at an AS concentration of 300 mM, where we might expect three peaks for NADH oxidase dimer, Prx decamer, and their complex. However, this is in agreement with the Gilbert–Jenkins theory [22,23] of a reversibly associating system, which states that the peak to the right is actually a reaction boundary, where the three aforementioned molecular species co-sediment and form one peak in $c(s)$. The results supported the conclusion from SPR and DLS that NADH oxidase and Prx form a weakly interacting complex, depending on the ionic strength. In fact, the peak for the reaction boundary was enhanced by increasing the concentration of Prx from 7 μ M up to 70 μ M, while the NADH oxidase peak decreased. The peak for NADH oxidase nearly diminished at the NADH oxidase to Prx ratio of 7 μ M: 70 μ M at 300 mM AS. Some decrease in the s -value of the reaction boundary with increasing concentration of Prx is very likely due to non-ideality (data not shown).

2.5. Structural analysis by small-angle X-ray scattering (SAXS)

We attempted to analyze the solution structures of the NADH oxidase–Prx complex following that of NADH oxidase and Prx by SAXS based on the best complex-forming condition found by AUC analysis (300 mM AS, NADH oxidase: Prx = 1:10; subunit per subunit). The structure image of Prx could not be observed in the absence of AS because the probable SAXS curve was obtained for its strong intermolecular force (data not shown), while its ring-shaped structure (presumed to be a decamer) arose in the presence of 300 mM AS. These data confirmed the result of crystallography of *A. xylanus* Prx (Fig. 6A) [20,21].

The image of NADH oxidase observed in solution appeared U-shaped (Fig. 6B). Although the X-ray crystallographic analysis of *A. xylanus* NADH oxidase has not yet been conducted, that of *S. typhimurium* AhpF, which belongs to the same family as NADH oxidase and exhibits a 51.2% shared identity [3], has already been analyzed (PDB code: 1HYU) [24]. Though the AhpF is less reactive with oxygen compared to NADH oxidase, it can reduce peroxides at the same rate constant that the NADH oxidase does [4]. The steric structure of NADH oxidase observed by SAXS structurally differed from that of crystallographic AhpF. AhpF is a homodimer composed of 57 kDa subunits. Each subunit is composed of three domains: an N-terminal domain containing a disulfide (NTD), an FAD binding domain, and an NADH binding disulfide-containing domain (NADH/SS) [25,9]. The amino acid primary sequence of NADH oxidase also has these three domains. We attempted to fit three domains of AhpF to the SAXS image of NADH oxidase using the Coot program [26]. Both the FAD binding domain and the NADH/SS domain of subunits remained fixed; only the NTD domains connected to the FAD binding domain by a flexible linker were moved manually to fit in the image, resulting in a good correspondence (Fig. 6C). Wood et al. advocated that the hypothetical alternate conformation of AhpF that allows for the reduction of peroxides in the presence of Prx [24], and the solution structure of NADH oxidase observed in this study agree with this hypothesis.

The above results indicated that the SAXS method was effective for determining the solution structures of Prx and NADH oxidase.

We next analyzed the solution structure of the NADH oxidase–Prx complex using SAXS under specific conditions (300 mM AS, NADH oxidase: Prx = 1:10; subunit per subunit). Although the formation of the complex was not observed in the absence of AS, as was true in the results of DLS and AUC, an image of a new hetero-oligomer complex was visible in the presence of 300 mM AS (Fig. 6D–1), and a decameric Prx was nicely fitted into the ring-shaped structure of the complex using the Coot program (Fig. 6D–2). Thus, the complex formation was also confirmed structurally through this SAXS measurement. However, both the accurate binding ratio of the two distinct proteins forming the complex and its molecular mass remain unclear. To address these concerns, we are planning to measure the binding ratio between NADH oxidase and Prx and their molecular masses using static light scattering analysis. In addition, the intracellular concentration of these proteins will need to be calculated. Finally, we would like to determine the metabolic significance of NADH oxidase–Prx system in *A. xylanus* based on these data in the future.

3. Conclusion

NADH oxidase formed a dimer independent of the ionic strength, whereas it and Prx formed a hetero-oligomer complex with high peroxide-reductase activity dependent on the ionic strength, suggesting that the complex formation is a key event for its rapid reaction toward peroxides.

4. Materials and methods

4.1. Construction of mutated plasmids

Plasmid pNOH1850 designed for overexpression of the wild-type NADH oxidase gene was used to construct derivatives that expressed the variant enzymes (C128S, C131S, C128S/C131S and C480S) [8]. *Escherichia coli* MV1184 was used as a host to construct the variant pNOH1850. *E. coli* JM109 was used as a host for variant pNOH1850. *E. coli* MV1184 and JM109 were grown with shaking at 37 °C in 2 × YT and LB medium, respectively.

Plasmid pNOH1850 was digested with *SacI*/*Bam*HI for C128S, C131S and C128S/C131S and with *SacI*/*Hind*III for C480S. The digested fragment was ligated into pBluescript or pUC119, from which were cleaved the corresponding restriction enzymes. Each resulting plasmid was transformed into *E. coli* MV1184 to obtain the single-stranded DNA [17]. The site-directed mutagenesis was performed by means of the single-stranded DNA as the template, following the mutagenic oligonucleotides and Sculptor IVM system according to the supplier's instructions (Amersham, RPN, 1526).

C128S: 5'-GGACAGTTTGGACTAGTTAAACTACGT-3'

C131S: 5'-GTTAGTTTAAACATGTCAAACCTCCGGATCTTGTGTTCAA-3'

C128S/C131S: 5'-GTTAGTTTAAACATCTCAAACCTCCAGATCTTGTGTTCAA-3'

C480S: 5'-GACGACCACTGTCATGACTGTGCGGAATGTT-3'

Double-stranded circular DNA from the mutagenesis reactions was transformed into *E. coli* JM109.

4.2. Purification of enzymes

NADH oxidase and Prx from *A. xylanus* were isolated as described previously [5].

E. coli JM109, which expressed the variant enzyme, was obtained using a previous method [17]. All variant enzymes were purified by a same method as that described below, and all of the following steps of the purification procedures were carried out at 4 °C. Crude extract was prepared by the method described previously except for disrupting the cells in a French pressure cell

(AMINCO) [17]. The crude extract was applied to a column DE52 (3.5 × 31 cm) equilibrated in 50 mM sodium phosphate buffer (pH 7.0) containing 0.5 mM EDTA. The column was washed with this same buffer, and the variant enzyme was eluted by 2000 mL of 250 mM sodium phosphate buffer (pH 7.0) containing 0.5 mM EDTA. Solid ammonium sulfate was added to the pool of variant enzyme to give a final concentration of 0.95 M, and the solution was stirred for 30 min. After the solution was centrifuged at 31,000 × g for 10 min, the supernatant was applied to a column Butyl TOYOPEARL 650S (2.5 × 18.5 cm) equilibrated in 50 mM sodium phosphate buffer (pH 7.0) containing 0.5 mM EDTA and 1.02 M ammonium sulfate. The column was washed with this same buffer, and the variant enzyme was eluted by 2000 mL linear gradient (from 1.02 M to 0 M ammonium sulfate). The eluted fraction was concentrated to about 10 mL by ultrafiltration (molecular weight cutoff 50,000, Advantec), and this solution was applied to a column TOYOPEARL HW-60S (2 × 91 cm) equilibrated in 50 mM sodium phosphate buffer (pH 7.0) containing 0.5 mM EDTA. The variant enzyme was eluted with this same buffer.

4.3. Extinction coefficient determination

The extinction coefficient of the protein bound FAD at 450 nm was determined for each of the variant enzymes by resolving the FAD from the protein and quantitating the free FAD. The spectra of samples of four variant proteins in 50 mM sodium phosphate buffer (pH 7.0) containing 0.5 mM EDTA were obtained. The FAD was then released by the addition of 0.1% SDS (final concentration) at room temperature for 30 min [8]. The extinction coefficients of four variant proteins were determined as follows:

C128S: $\epsilon_{450} = 13,100 \text{ M}^{-1} \text{ cm}^{-1}$, C131S: $\epsilon_{450} = 12,990 \text{ M}^{-1} \text{ cm}^{-1}$, C128S/C131S: $\epsilon_{450} = 12,900 \text{ M}^{-1} \text{ cm}^{-1}$, C480S: $\epsilon_{450} = 13,200 \text{ M}^{-1} \text{ cm}^{-1}$.

4.4. NADH peroxidase activity for hydrogen peroxide of variant NADH oxidase

The hydrogen peroxide reductase activity of wild-type or variant NADH oxidases in the presence of Prx was measured using a stopped-flow spectrophotometer as described previously [4]. The composition of reaction mixture was also the same as that of previous experiments [4]. We previously assayed the activity of the enzyme system under anaerobic conditions; in this experiment, we did so under aerobic conditions. In the presence of Prx, the peroxide reductase activities were the same in air-saturated solution as were those determined anaerobically [4].

4.5. Surface plasmon resonance (SPR)

Studies were performed using a BIAcore J apparatus (BIAcore AB, Uppsala, Sweden). Prx was covalently coupled via primary amino groups on a CM5 sensor chip via standard N-hydroxysuccinimide and N-ethyl-N-(3-(dimethylamino)propyl) carbodiimide activation. Another flow cell for use as a control was subjected to the identical immobilization procedure in the absence of protein. The association of NADH oxidase with immobilized Prx (approximately 5000 RU) was studied by injection of varying concentrations of NADH oxidase at 25 °C for 360 s in a running buffer (50 mM HEPES buffer, pH 7.0, 100 mM AS) at a flow rate of 30 $\mu\text{L}/\text{min}$. Dissociation of the NADH oxidase–Prx complex was then observed in the running buffer. Data analysis was performed using BIAevaluation software 3.2 (BIAcore AB).

4.6. Dynamic light scattering (DLS)

DLS measurements were performed using DynaPro-99 operated with the program DYNAMICS (Protein Solution, USA) to estimate

the molecular mass of *A. xylanus* NADH oxidase, Prx, and their mixture in solution at various concentrations of AS. Samples of NADH oxidase (13 μM), Prx (13 μM), and their mixture in various ratios from 1:1 to 1:10 (subunit per subunit) in 50 mM HEPES–NaOH buffer (pH 7.0) with various concentrations of AS from 0 mM to 320 mM were prepared in 100 μL aliquots and filtered through a 0.02 μm membrane (Whatman Int.). Protein samples were loaded into sample cells previously equilibrated with buffer solutions containing salt (AS) and illuminated with a solid-state laser at 25 °C. The D_T measurements were repeated 20 times and averaged for each sample. R_H is derived from D_T by the Stokes–Einstein equation (Eq. (1)).

$$R_H = kT/6\pi\eta D_T \quad (1)$$

where k , T , and η are the Boltzmann constant, absolute temperature, and viscosity, respectively. As R_H is sensitive to the viscosity η of the solution, the influence of salt at each concentration on η was corrected by applying the viscosity of protein-free salt solutions (data not shown). Finally, the molecular mass of *A. xylanus* NADH oxidase, Prx, and the mixture of NADH oxidase and Prx were calculated from R_H using DYNAMICS, which includes a standard curve for globular proteins.

4.7. Analytical ultracentrifugation (AUC)

Sedimentation velocity experiments were carried out using an Optima XL-I analytical ultracentrifuge (Beckman–Coulter) with an eight-hole An50Ti rotor at 20 °C. Before centrifugation, NADH oxidase and Prx solutions at the specified concentration ratios were dialyzed overnight against buffer solutions with a specified concentration of AS in the presence of 50 mM phosphate buffer at pH 7.0. Each sample was then transferred into a 12-mm double-sector Epon cell and centrifuged at a rotor speed of 40,000 rpm. The concentrations were monitored at 280 nm. The sedimentation velocity data were analyzed using the SEDFIT program [27].

4.8. Small-angle X-ray scattering (SAXS)

Approximately 200 μL of purified NADH oxidase and Prx (200 μM and 3 mM, respectively) were injected into 10,000 MWCO cassette membranes (Thermo scientific Inc.), and dialyzed against 1 L of 50 mM HEPES–NaOH buffer (pH 7.0) containing 300 mM AS at 4 °C for 180 min. The dialysis solutions of both proteins were centrifuged at 15,000 rpm for 15 min at 4 °C and supernatants were collected as measurement samples. The protein solution of NADH oxidase and Prx were prepared at concentrations of 1.79, 7.15 and 14.3 mg/mL by using each extinction coefficient and molecular mass (NADH oxidase: $\epsilon_{450} = 13,200 \text{ M}^{-1} \text{ cm}^{-1}$, MW = 54,977 g/mol, Prx: $\epsilon_{280} = 25,800 \text{ M}^{-1} \text{ cm}^{-1}$, MW = 20,774 g/mol). Samples of NADH oxidase–Prx complex were also prepared at concentrations of 1.79, 7.15 and 14.3 mg/mL by mixing a two-protein solution at a ratio of NADH oxidase: Prx = 1:5 (subunit per subunit). The radius of gyration (R_g) of NADH oxidase, Prx, and their complex determined using the program PRIMUS [29] were not affected by the tested protein solutions (Fig. S1), and therefore the complex sample mixture of two proteins solutions at a ratio of NADH oxidase: Prx = 1:10 (subunit per subunit) was prepared only at a concentration of 14.3 mg/mL. SAXS measurements were carried out on a Rigaku BioSAXS-1000 using 30 μL of samples. A total of eight (or twelve) data sets were collected after 120 (or 180) min of exposure (15 min per data set). The final scattering curve was averaged from eight (or twelve) data sets with the program SAXSLab (Rigaku). Subsequent data were analyzed by the ATSAS program Package [28]. The scattering curve derived from protein was obtained by processing the averaged data using the

program PRIMUS [29] (Figs. S2A–S5A). The R_g value was determined by Guinier plot analysis [29] (Figs. S2B–S5B). The particle distance distribution function and maximum particle dimension (D_{\max}) were determined using the GNOM program [30]. Based on the scattering curve, the protein structure was reconstructed through an ensemble of dummy residues (C- α atoms of amino acid residues) using the GASBOR program [31]. The protein structure was determined after eight GASBOR models were averaged using the DAMAVER program [32].

4.9. Modeling of NADH oxidase

The structure of NADH oxidase was manually built based on the crystal structure of AhpF (PDB entry 1HYU) [24] using the Coot program [26]. AhpF is a homodimer containing 1 mol FAD per subunit, and the N-terminal domain (residues 1–196) is connected to the C-terminal portion (residues 210–521) with the flexible linker (residues 197–209) [24,25,9]. We split a subunit into a C-terminal domain and an N-terminal portion. Then, we moved the N-terminal domain to fit into the SAXS image of NADH oxidase while maintaining the closeness of the domain junctions.

Author contributions

T. A., Y. N., S. Kawasaki and J. S. purified enzymes. T. Z. conducted SPR measurements. M. O. and M. Y. analyzed the data of SPR. T. A. measured enzyme activities and conducted DLS experiments. F. A. conducted AUC experiments, and F. A., S. Kanamaru and T. A. analyzed the data of AUC experiments. T. M. acquired the data of protein structure by SAXS. T. M., D. M., S. Kimata, K. H. and S. Y. analyzed the data of SAXS measurements. S. Y. and S. Kimata modeled protein structures. Y. N. conducted this research. Y. N. and S. Kimata wrote the paper.

Acknowledgments

We thank Dr. Ken Kitano of the Nara Institute of Science and Technology for valuable advice about protein structures. We also thank Masato Date, Akihiro Satoh, and Shinya Tatsumi of the Tokyo University of Agriculture for helpful technical assistance in elemental experiments of SPR and DLS.

Appendix A. Supplementary data

Supplementary data associated with this article can be found, in the online version, at <http://dx.doi.org/10.1016/j.fob.2015.01.005>.

References

- [1] Niimura, Y., Koh, E., Yanagida, F., Suzuki, K.I., Komagata, K. and Kozaki, M. (1990) *Amphibacillus xylanus* gen.-nov., sp.-nov., a facultatively anaerobic spore-forming xylan-digesting bacterium which lacks cytochrome, quinone, and catalase. *Int. J. Syst. Bacteriol.* 40, 297–301.
- [2] Niimura, Y., Koh, E., Uchimura, T., Ohara, N. and Kozaki, M. (1989) Aerobic and anaerobic metabolism in a facultative anaerobic Ep01 lacking cytochrome, quinone and catalase. *FEMS Microbiol. Lett.* 61, 79–84.
- [3] Niimura, Y., Ohnishi, K., Yaritha, Y., Hidaka, M., Masaki, H., Uchimura, T., Suzuki, H. and Kozaki, M. (1993) A flavoprotein functional as NADH oxidase from *Amphibacillus xylanus* Ep01: purification and characterization of the enzyme and structural analysis of its gene. *J. Bacteriol.* 175, 7945–7950.
- [4] Niimura, Y., Poole, L.B. and Massey, V. (1995) *Amphibacillus xylanus* NADH oxidase and *Salmonella typhimurium* alkyl-hydroperoxide reductase flavoprotein components show extremely high scavenging hydroperoxide reductase 22-kDa protein component. *J. Biol. Chem.* 270, 25645–25650.
- [5] Niimura, Y., Nishiyama, Y., Saito, D., Tsuji, H., Hidaka, M., Miyaji, T., Watanabe, T. and Massey, V. (2000) A hydrogen peroxide-forming NADH oxidase that functions as an alkyl hydroperoxide reductase in *Amphibacillus xylanus*. *J. Bacteriol.* 182, 5046–5051.
- [6] Mochizuki, D., Arai, T., Asano, M., Sasakura, N., Watanabe, T., Shiwa, Y., Nakamura, S., Katano, Y., Fujinami, S., Fujita, N., Abe, A., Sato, J., Nakagawa, J. and Niimura, Y. (2014) Adaptive response of *Amphibacillus xylanus* to normal aerobic and forced oxidative stress conditions. *Microbiology* 160, 340–352.
- [7] Mochizuki, D., Tanaka, N., Ishikawa, M., Endo, A., Shiwa, Y., Fujita, N., Sato, J. and Niimura, Y. (2012) Evolution and diversification of oxygen metabolism of aerotolerant anaerobes in the order Bacillales and other bacterial taxonomic groups. *The Bulletin of BISMis* 3, 1–17.
- [8] Ohnishi, K., Niimura, Y., Yokoyama, K., Hidaka, M., Masaki, H., Uchimura, T., Suzuki, H., Uozumi, T., Kozaki, M., Komagata, K. and Nishino, T. (1994) Purification and analysis of a flavoprotein functional as NADH oxidase from *Amphibacillus xylanus* overexpressed in *Escherichia coli*. *J. Biol. Chem.* 269, 31418–31423.
- [9] Tartaglia, L.A., Storz, G., Brodsky, M.H., Lai, A. and Ames, B.N. (1990) Alkyl hydroperoxide reductase from *Salmonella typhimurium*. Sequence and homology to thioredoxin reductase and other flavoprotein disulfide oxidoreductases. *J. Biol. Chem.* 265, 10535–10540.
- [10] Niimura, Y. and Massey, V. (1996) Reaction mechanism of *Amphibacillus xylanus* NADH oxidase/alkyl hydroperoxide reductase flavoprotein. *J. Biol. Chem.* 271, 30459–30464.
- [11] Ogura, Y. (1955) Catalase activity at high concentration of hydrogen peroxide. *Arch. Biochem. Biophys.* 57, 288–300.
- [12] Little, C. (1972) Steroid hydroperoxides as substrates for glutathione peroxidase. *Biochim. Biophys. Acta* 284, 375–381.
- [13] Chaudiere, J. and Tapple, A.L. (1983) Purification and characterization of selenium–glutathione peroxidase from hamster liver. *Arch. Biochem. Biophys.* 226, 448–457.
- [14] Takahashi, K., Avissar, N., Whitin, J. and Cohen, H. (1987) Purification and characterization of human plasma glutathione peroxidase: a selenoglycoprotein distinct from the known cellular enzyme. *Arch. Biochem. Biophys.* 256, 677–686.
- [15] Flohe, L., Loschen, G., Günzler, W.A. and Eichele, E. (1972) Glutathione peroxidase, V. Hoppe-Seyler's Z. *Physiol. Chem.* 353, 987–999.
- [16] Björnstedt, M., Xue, J., Huang, W., Åkesson, B. and Holmgren, A. (1994) The thioredoxin and glutaredoxin systems are efficient electron donors to human plasma glutathione peroxidase. *J. Biol. Chem.* 269, 29382–29384.
- [17] Ohnishi, K., Niimura, Y., Hidaka, M., Masaki, H., Suzuki, H., Uozumi, T. and Nishino, T. (1995) Role of cysteine 337 and cysteine 340 in flavoprotein that functions as NADH oxidase from *Amphibacillus xylanus* studied site-directed mutagenesis. *J. Biol. Chem.* 270 (11), 5812–5817.
- [18] Ellis, H.R. and Poole, L.B. (1997) Role for the two cysteine residue of AhpF in catalysis of peroxide reduction by alkyl hydroperoxide reductase from *Salmonella typhimurium*. *Biochemistry* 36, 13349–13356.
- [19] Calzi, M.L. and Poole, L.B. (1997) Requirement of the two AhpF cysteine disulfide centers in catalysis of peroxide reduction by alkyl hydroperoxide reductase. *Biochemistry* 36, 13357–13364.
- [20] Kitano, K., Niimura, Y., Nishiyama, Y. and Miki, K. (1999) Stimulation of peroxidase activity by decamerization related to ionic strength: AhpC protein from *Amphibacillus xylanus*. *J. Biochem.* 126, 313–319.
- [21] Kitano, K., Kita, A., Hakoshima, T., Niimura, Y. and Miki, K. (2005) Crystal structure of decameric peroxidoredoxin (AhpC) from *Amphibacillus xylanus*. *Proteins* 59, 644–647.
- [22] Suchuck, P. (2010) Diffusion of the reaction boundary of rapidly interacting macromolecules in sedimentation velocity. *Biophys. J.* 98, 2741–2751.
- [23] Gilbert, G.A. and Jenkins, R.C. (1956) Boundary problems in the sedimentation and electrophoresis of complex systems in rapid reversible equilibrium. *Nature* 177, 853–854.
- [24] Wood, Z.A., Poole, L.B. and Karplus, A. (2001) Structure of intact AhpF reveals a mirrored thioredoxin-like active site and implies large domain rotations during catalysis. *Biochemistry* 40, 3900–3911.
- [25] Poole, L.B. (1996) Flavin-dependent alkyl hydroperoxide reductase from *Salmonella typhimurium*. 2. Cystine disulfides involved in catalysis of peroxide reduction. *Biochemistry* 35, 65–75.
- [26] Emsley, P. and Cowtan, K. (2004) Coot: model-building tools for molecular graphics. *Acta Crystallogr. D* 60, 2126–2132.
- [27] Schuck, P. (2000) Size-distribution analysis of macromolecules by sedimentation velocity ultracentrifugation and lamm equation modeling. *Biophys. J.* 78, 1606–1619.
- [28] Petoukhov, M.V., Konarev, P.V., Kikhney, A.G. and Svergun, D.I. (2007) ATSAS 2.1-towards automated and web-supported small-angle scattering data analysis. *J. Appl. Crystallogr.* 40, s223–s228.
- [29] Konarev, P.V., Volkov, V.V., Sokolova, A.V., Koch, M.H.J. and Svergun, D.I. (2003) PRIMUS – a Windows-PC based system for small-angle scattering data analysis. *J. Appl. Crystallogr.* 36, 1277–1282.
- [30] Svergun, D.I. (1992) Determination of the regularization parameter in indirect-transform methods using perceptual criteria. *J. Appl. Crystallogr.* 25, 495–503.
- [31] Svergun, D.V., Petoukhov, M.V. and Koch, M.H.J. (2001) Determination of domain structure of proteins from X-ray solution scattering. *Biophys. J.* 80, 2946–2953.
- [32] Volkov, V.V. and Svergun, D.I. (2003) Uniqueness of ab-initio shape determination in small-angle scattering. *J. Appl. Crystallogr.* 36, 860–864.